

Forbidden oxygen lines in comets at various heliocentric distances[★]

A. Decock¹, E. Jehin¹, D. Hutsemékers¹, J. Manfroid¹

Institut d'Astrophysique et Géophysique et Océanographie, Université de Liège, Allée du 6 août 17, 4000 Liège, Belgium
e-mail: adcock@ulg.ac.be

Received Month, year; accepted Month, year

ABSTRACT

We present a study of the three forbidden oxygen lines [OI] located in the optical region (i.e., 5577.339 Å, 6300.304 Å and 6363.776 Å) in order to better understand the production of these atoms in cometary atmospheres. The analysis is based on 48 high-resolution and high signal-to-noise spectra collected with UVES at the ESO VLT between 2003 and 2011 referring to 12 comets of different origins observed at various heliocentric distances. The flux ratios I_{6300}/I_{6364} and $G/R = I_{5577}/(I_{6300} + I_{6364})$ are evaluated to determine the parent species of the oxygen atoms by comparison with theoretical models. This analysis confirms that, at around 1 AU, H₂O is the main parent molecule producing oxygen atoms. At heliocentric distances > 2.5 AU, the G/R ratio is changing rapidly, an indication that other molecules are starting to contribute. CO and CO₂, the most abundant species after H₂O in the coma, are good candidates and the G/R ratio is used to estimate their abundances. We found that the CO₂ abundance relative to H₂O in comet Q4 (NEAT) observed at 4 AU could be as high as ~70%. The intrinsic widths of the oxygen lines were also measured. The green line is in average about 1 km s⁻¹ broader than the red lines while the theory predicts the red lines should be broader. But at 4 AU, we found that the width of the green and red lines in comet Q4 (NEAT) are the same which could be explained if CO₂ is the main contributor.

Key words. Comets: general – Techniques: spectroscopic – Line: formation

1. Introduction

Comets are small bodies formed at the birth of the Solar system 4.6 billion years ago. Since they did not evolve much, they are potential witnesses of the physical and chemical processes at play at the beginning of our Solar system (Ehrenfreund & Charnley 2000). Their status of "fossils" gives them a unique role to understand the origins of the Solar system, not only from the physical and dynamical point of view but also from the chemical point of view (thanks to the knowledge of the compounds of the nucleus). When the comet gets closer to the Sun, the ices of the nucleus sublimate to form the coma (the comet atmosphere) where oxygen atoms are detected. Oxygen is an important element in the chemistry of the Solar system given its abundance and its presence in many molecules including H₂O which constitutes 80% of the cometary ices. Oxygen atoms are produced by the photo-dissociation of molecules coming from the sublimation of the cometary ices. Chemical reactions Eq.(1) to (6) involve possible parent molecules (Bhardwaj & Raghuram 2012; Festou & Feldman 1981).



[★] Based on observations made with ESO Telescope at the La Silla Paranal Observatory under programs ID 268.C-5570, 270.C-5043, 073.C-0525, 274.C-5015, 075.C-0355, 080.C-0615, 280.C-5053, 086.C-0958 and 087.C-0929.



Oxygen atoms have been detected in comets through the three forbidden lines observed in emission at 5577.339 Å (the green line), 6300.304 Å and 6363.776 Å (the red lines) (Swings 1962). These lines are coming from the deexcitation of the upper state (2p⁴)¹S₀ to the (2p⁴)¹D₂ state for the 5577.339 Å line and from the (2p⁴)¹D₂ state to the (2p⁴)³P_{1,2} states for the doublet red lines (see Fig. 1). The green line measurement is more difficult owing to its fainter intensity and the many C₂ lines located around it. One of the first theoretical studies was carried out by Festou & Feldman (1981). They reviewed the production rate of O(¹S) and O(¹D) obtained in the laboratory from H₂O, CO and CO₂ photo-dissociations and measured the corresponding ¹S/¹D ratio. Recently, Bhardwaj & Raghuram (2012) made a new model for oxygen atom emissions and calculated the production rate of O(¹S) and O(¹D) for chemical reactions (1) to (6). The estimated ¹S/¹D ratios are significantly different from Festou & Feldman (1981) and are given in Table 1.

Up to now, little systematic researchwork has been done to study these lines at various heliocentric distances because the detection of the forbidden lines requires both high spectral and high spatial resolutions. Morrison et al. (1997) observed oxygen in comet C/1996 B2 (Hyakutake) with the 1-m Ritter Observatory telescope, Cochran & Cochran (2001) and Cochran (2008) analysed [OI] lines in the spectra of 8 comets observed at the McDonald Observatory (see Bhardwaj & Raghuram (2012) for a complete review of these measurements). The present paper reports the results obtained for a homogeneous set of high quality spectra of 12 comets of various origins observed since 2003 with

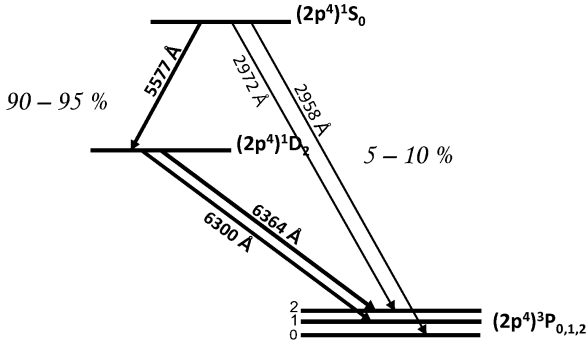


Fig. 1. Energy level diagram for [OI] lines.

Parents	Production rate (s^{-1})		Ratio	
	O(1S)	O(1D)	$^1S/^1D$	$^1S/^1D^a$
H ₂ O	$6.4 \cdot 10^{-8}$	$8.0 \cdot 10^{-7}$	0.080	~ 0.1
CO	$4.0 \cdot 10^{-8b}$	$5.1 \cdot 10^{-8}$	0.784	~ 1
CO ₂	$7.2 \cdot 10^{-7}$	$1.2 \cdot 10^{-6}$	0.600	~ 1

Table 1. The production rates and $^1S/^1D$ ratios obtained by Bhardwaj & Raghuram (2012) for photo-dissociation reactions at 1 AU.

^a The ratios obtained by Festou & Feldman (1981) are given in the last column for comparison.

^b This rate comes from Huebner & Carpenter (1979).

UVES mounted on one of the 8-m telescope of the ESO VLT. First, we measured the intensities of the three forbidden oxygen lines. Two ratios were evaluated : the ratio between the two red lines, I_{6300}/I_{6364} , and the ratio of the green line to the sum of the red lines, $I_{5577}/(I_{6300} + I_{6364})$ which we shall denote as G/R hereafter. The purpose of the latter is to determine the main parent molecule of the oxygen atoms by comparing our results with the Bhardwaj & Raghuram (2012) effective excitation rates. We also observed how the G/R ratio depends on the heliocentric distance by analysing spectra of comets C/2001 Q4 (NEAT) and C/2009 P1 (Garradd) at small and large distances from the Sun. Finally, we measured the Full Width at Half Maximum (FWHM) of the three lines. There is a long-standing debate on the FWHM measurement because the first observations made by Cochran (2008) are in contradiction with the theory. The intrinsic width of the green line is wider than the red ones while the theory predicts the opposite (Festou 1981).

2. Observations

Our analysis is based on 12 comets listed in Table 2, considering the two components of 73P/Schwassmann-Wachmann 3 (B and C) as two comets. This sample is characterized by a large diversity. These comets have various dynamical origins (external, new, Jupiter family, Halley type) and are observed at different heliocentric distances (from 0.68 AU to 3.73 AU). Some are split comets like 73P/SW3 or did a close approach to Earth. Others have been observed at large heliocentric distances like Q4 (NEAT) and P1 (Garradd). The observing material is made of a selection of 48 high signal-to-noise spectra obtained during the last ten years (Manfroid et al. (2009) ; Jehin et al. (2009) and references therein) with the cross-dispersed echelle spectrograph UVES (Dekker et al. 2000). A dichroic splits the light beam into two arms (3000 to 5000 Å and 4200 to 11000 Å). In most observations, a slit of $0.45'' \times 11''$ was used. With such a slit, the resolving power is $R = \lambda/\Delta\lambda = 110000$ in the red arm.

All spectra were recorded with nearly the same instrumental setting. Such a high resolution is needed to isolate the [OI] emission lines from the telluric lines and other cometary lines (C₂, NH₂) (see Fig.2). The slit was always centered on the cometary nucleus. For a comet located at 1 AU from the Earth, the spatial area covered by the slit is approximatively 320 km by 8000 km. The size of the slit for each individual spectrum is given in Table 3.

3. Data reduction

The 2D spectra were reduced with the UVES pipeline reduction program. For data obtained until 2008, the UVES pipeline (version 2.8.0) was used within the ESO-MIDAS environment to extract, for each order separately, the 2D spectra, bias-subtracted, flat-fielded and wavelength calibrated. ESO-MIDAS is a special software containing packages to reduce ESO data¹. For a given setting, the orders were then merged using a weighting scheme to correct for the blaze function, computed from high S/N master flat-fields reduced in exactly the same way. This procedure leads to a good order merging. The post-2008 observations were reduced with the gasgano CPL² interface (version 2.4.3) of the re-furbished UVES pipeline that directly provides accurately merged 2D spectra. 1D spectra were extracted by averaging the 2D ones, with cosmic rejection. Standard stars were similarly reduced and combined to derive instrumental response functions used to correct the 1D spectra. The wavelength calibration was computed using Thorium Argon (Th-Ar) spectra. The calibration revealed small shifts of the lines due to the fact that the Th-Ar spectra were usually taken in the day and not right after the comet observations. This shift was removed using 9 cometary lines of NH₂ in the vicinity of the red [OI] lines and for which laboratory wavelengths are well known.

Before doing any measurement, the telluric absorption lines were removed and the solar continuum contribution subtracted using the BAAS and Kurucz spectra. These two spectra are solar spectra, with atmospheric lines for the BAAS³ spectrum and without for the Kurucz⁴ one (2005). Around the red doublet line at 6300 Å, there are indeed telluric absorption lines mostly due to O₂ molecules in the Earth's atmosphere which could lead to an underestimate of the forbidden oxygen line intensity (see Fig. 3).

The Solar continuum has three contributions. First and foremost is the one due to the reflection of sunlight on the dust particles in the coma. Another one appears when the observations are made in or close to the twilight. A third contribution is, in a few cases, the background radiation by the Moon. To remove these contaminations, we Doppler shifted the BAAS spectrum to the proper values and scaled the intensities until the solar features are completely removed. This provides the final spectrum such as the one presented in Fig. 4 for comet 8P/Tuttle, free of any solar and telluric lines.

4. Data analysis

After the reduction and the correction of the data, we measured both the intensity and the FWHM of the three forbidden oxygen lines by fitting a gaussian profile using the IRAF⁵ software.

¹ <http://www.eso.org/sci/software/esomidas/>

² <http://www.eso.org/sci/software/gasgano/>

³ http://bass2000.obspm.fr/solar_spect.php

⁴ <http://kurucz.harvard.edu/sun/irradiance2005/irradthu.dat>

⁵ IRAF is a tool for the reduction and the analysis of astronomical data (<http://iraf.noao.edu>).

Comet	Short name comet	T_p	e	a	q	i	P	T_J	Type (L)
C/2002 V1 (NEAT)	V1 (NEAT)	18-02-2003	0.99990	1010	0.10	82	32100	0.06	EXT
C/2002 X5 (Kudo-Fujikawa)	X5 (Kudo-Fujikawa)	29-01-2003	0.99984	1175	0.19	94	40300	-0.03	EXT
C/2002 Y1 (Juels-Holvorcem)	Y1 (Juels-Holvorcem)	13-04-2003	0.99715	250.6	0.71	104	3967	-0.23	EXT
C/2001 Q4 (NEAT)	Q4 (NEAT)	16-05-2004	1.00069	-	0.96	100	-	-	NEW
C/2002 T7 (LINEAR)	T7 (LINEAR)	23-04-2004	1.00048	-	0.61	161	-	-	NEW
C/2003 K4 (LINEAR)	K4 (LINEAR)	14-10-2004	1.00030	-	1.02	134	-	-	NEW
9P/Tempel 1	Tempel 1	05-07-2005	0.51749	3.1	1.51	11	5.5	2.97	JF
73P-C/Schwassmann-Wachmann 3	SWc3	07-06-2006	0.69338	3.1	0.94	11	5.4	2.78	JF
73P-B/Schwassmann-Wachmann 3	SWb3	08-06-2006	0.69350	3.1	0.94	11	5.4	2.78	JF
8P/Tuttle	Tuttle	27-01-2008	0.8198	5.7	1.03	55	13.6	1.60	HF
103P/Hartley 2	Hartley 2	28-10-2010	0.6950	3.5	1.06	14	6.5	2.64	JF
C/2009 P1 (Garradd)	P1 (Garradd)	23-12-2011	1.0011	-	1.55	106	-	-	NEW

Table 2. Orbital characteristics of the 12 comets and their classification. T_p is the epoch of the perihelion (dd-mm-yyyy), e the eccentricity, a is related to the semi-major axis of the orbit (AU), q is the perihelion distance (AU), i represents the inclination on the ecliptic (degrees), P is the period (years), T_J is the Tisserand parameter relative to Jupiter. The last data correspond to the classification of the comets according to Levison (1996) : HF and JF mean "Halley Family" and "Jupiter family" and gather comets with short period (< 200 years) ; EXT and NEW are respectively for external comets ($a < 10000$ AU) and new comets ($a > 10000$ AU) which directly come from the Oort Cloud.

Comet	MJD	r (AU)	\dot{r} (km s ⁻¹)	Δ (AU)	$\dot{\Delta}$ (km s ⁻¹)	Exptime (s)	Slit (″×″)
C/2002 V1 (NEAT)	2 647.037	1.22	-36.51	0.83	7.88	2100	0.45 × 11.00
C/2002 V1 (NEAT)	2 647.062	1.22	-36.53	0.83	7.99	2100	0.45 × 11.00
C/2002 V1 (NEAT)	2 649.031	1.18	-37.11	0.84	8.29	2100	0.45 × 11.00
C/2002 V1 (NEAT)	2 649.056	1.18	-37.11	0.84	8.33	1987	0.45 × 11.00
C/2002 V1 (NEAT)	2 719.985	1.01	39.76	0.63	42.02	600	0.45 × 11.00
C/2002 X5 (Kudo-Fujikawa)	2 705.017	1.06	37.01	0.99	29.34	1800	0.45 × 11.00
C/2002 X5 (Kudo-Fujikawa)	2 705.039	1.07	37.00	0.99	29.40	1800	0.45 × 11.00
C/2002 X5 (Kudo-Fujikawa)	2 705.060	1.07	36.99	0.99	29.45	1800	0.45 × 11.00
C/2002 Y1 (Juels-Holvorcem)	2 788.395	1.14	24.09	1.56	-7.24	1800	0.40 × 11.00
C/2002 Y1 (Juels-Holvorcem)	2 788.416	1.14	24.09	1.56	-7.21	1800	0.40 × 11.00
C/2002 Y1 (Juels-Holvorcem)	2 789.394	1.16	24.18	1.55	-7.21	1800	0.40 × 11.00
C/2002 Y1 (Juels-Holvorcem)	2 789.415	1.16	24.19	1.55	-7.18	1800	0.40 × 11.00
C/2001 Q4 (NEAT)	2 883.293	3.73	-18.80	3.45	-25.42	4500	0.45 × 11.00
C/2001 Q4 (NEAT)	2 883.349	3.73	-18.80	3.45	-25.32	4500	0.45 × 11.00
C/2001 Q4 (NEAT)	2 889.236	3.67	-18.91	3.36	-23.67	7200	0.45 × 11.00
C/2001 Q4 (NEAT)	2 889.320	3.66	-18.91	3.36	-23.54	7200	0.45 × 11.00
C/2002 T7 (LINEAR)	3 131.421	0.68	15.83	0.61	-65.62	1080	0.44 × 12.00
C/2002 T7 (LINEAR)	3 151.976	0.94	25.58	0.41	54.98	2678	0.30 × 12.00
C/2002 T7 (LINEAR)	3 152.036	0.94	25.59	0.42	55.20	1800	0.30 × 12.00
C/2003 K4 (LINEAR)	3 131.342	2.61	-20.34	2.37	-43.12	4946	0.80 × 11.00
C/2003 K4 (LINEAR)	3 132.343	2.59	-20.35	2.35	-42.95	4380	0.60 × 11.00
C/2003 K4 (LINEAR)	3 329.344	1.20	14.81	1.51	-28.23	1500	0.44 × 12.00
9P/Tempel 1	3 553.955	1.51	-0.21	0.89	8.95	7200	0.44 × 12.00
9P/Tempel 1	3 554.954	1.51	-0.15	0.89	9.07	7200	0.44 × 12.00
9P/Tempel 1	3 555.955	1.51	-0.04	0.90	9.19	7200	0.44 × 12.00
9P/Tempel 1	3 557.007	1.51	0.09	0.90	9.48	9600	0.44 × 12.00
9P/Tempel 1	3 557.955	1.51	0.20	0.91	9.44	7500	0.44 × 12.00
9P/Tempel 1	3 558.952	1.51	0.31	0.91	9.55	7500	0.44 × 12.00
9P/Tempel 1	3 559.954	1.51	0.43	0.92	9.68	7500	0.44 × 12.00
9P/Tempel 1	3 560.952	1.51	0.55	0.93	9.80	7800	0.44 × 12.00
9P/Tempel 1	3 561.953	1.51	0.66	0.93	9.91	7200	0.44 × 12.00
9P/Tempel 1	3 562.956	1.51	0.78	0.94	10.04	7200	0.44 × 12.00
73P-C/SW 3	3 882.367	0.95	-4.17	0.15	12.31	4800	0.60 × 12.00
73P-B/SW 3	3 898.369	0.94	1.79	0.25	13.10	4800	0.60 × 12.00
8P/Tuttle	4 481.021	1.04	-4.29	0.36	21.64	3600	0.44 × 10.00
8P/Tuttle	4 493.018	1.03	0.40	0.52	24.72	3900	0.44 × 10.00
8P/Tuttle	4 500.017	1.03	3.16	0.62	24.16	3900	0.44 × 10.00
103P/Hartley 2	5 505.288	1.06	2.53	0.16	7.08	2900	0.44 × 12.00
103P/Hartley 2	5 505.328	1.06	2.55	0.16	7.19	3200	0.44 × 12.00
103P/Hartley 2	5 510.287	1.07	4.05	0.18	7.96	2900	0.44 × 12.00
103P/Hartley 2	5 510.328	1.07	4.07	0.18	8.07	3200	0.44 × 12.00
103P/Hartley 2	5 511.363	1.08	4.37	0.19	8.27	900	0.44 × 12.00
C/2009 P1 (Garradd)	5 692.383	3.25	-16.91	3.50	-44.66	3600	0.44 × 12.00
C/2009 P1 (Garradd)	5 727.322	2.90	-16.89	2.57	-46.38	3600	0.44 × 12.00
C/2009 P1 (Garradd)	5 767.278	2.52	-16.46	1.64	-29.26	1800	0.44 × 12.00
C/2009 P1 (Garradd)	5 813.991	2.09	-14.82	1.47	14.79	4800	0.44 × 12.00
C/2009 P1 (Garradd)	5 814.974	2.08	-14.77	1.48	15.31	4800	0.44 × 12.00
C/2009 P1 (Garradd)	5 815.982	2.07	-14.71	1.49	15.84	4800	0.44 × 12.00

Table 3. Individual spectra. MJD = JD - 2 450 000.5 the Modified Julian Day, r is the heliocentric distance, Δ the geocentric distance. \dot{r} and $\dot{\Delta}$ are respectively the heliocentric and geocentric velocities. **Exptime** corresponds to the exposure time in seconds. **Slit** gives the size of the entrance slit of the spectrograph in arc seconds.

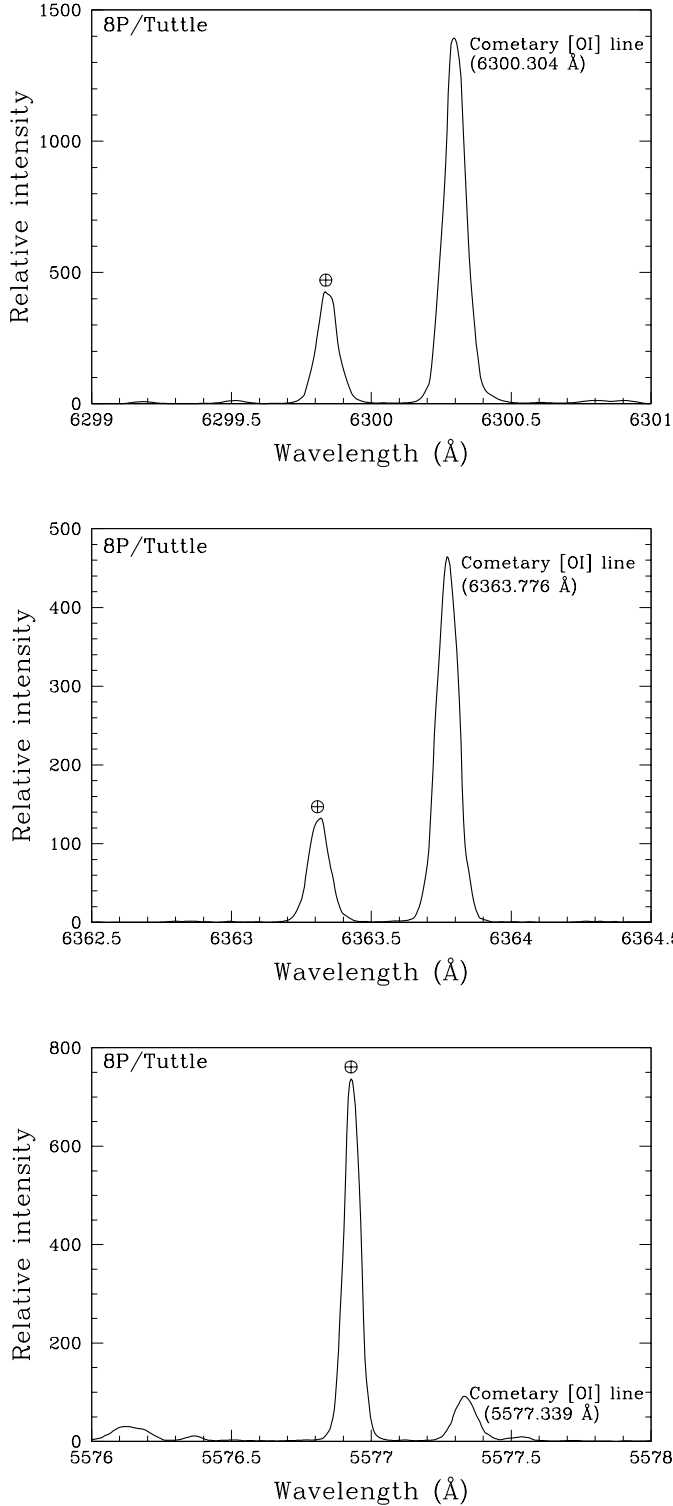


Fig. 2. The 6300.304 Å, 6363.776 Å and 5577.339 Å oxygen lines (telluric \oplus) and cometary) in a 3600s spectrum of comet 8P/Tuttle obtained in March 2008. Thanks to the high resolution of the UVES spectrograph, the cometary and telluric lines are well separated when the Doppler shift is larger than 15 km s⁻¹.

The observed width is the convolution of the instrumental profile with the natural width :

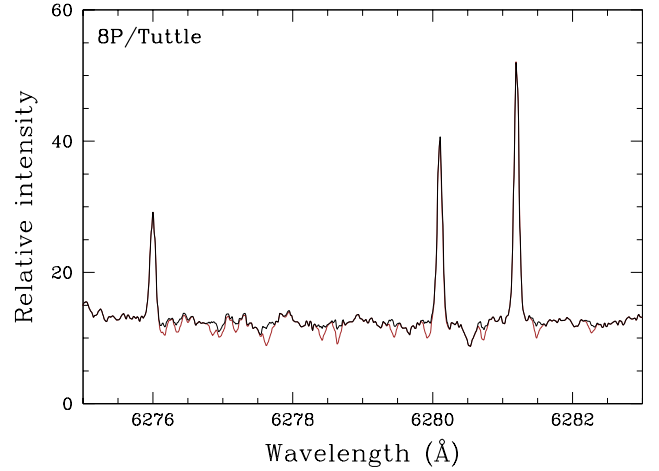


Fig. 3. The telluric absorption line correction in the vicinity of red [OI] lines. The black spectrum has been corrected (thick line), the red one is uncorrected.

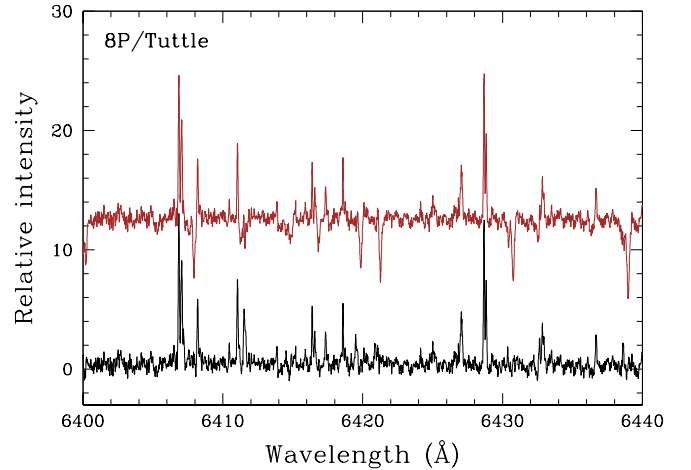


Fig. 4. The solar continuum subtraction in the vicinity of the red [OI] lines. The solar continuum has been removed in the lower spectrum (black) while it is present in the upper one (in red). It corresponds to the final spectrum on which the measurements of the [OI] will be made.

$$\text{FWHM}_{\text{observed}}(\lambda) = \sqrt{\text{FWHM}_{\text{intrinsic}}^2(\lambda) + \text{FWHM}_{\text{instrumental}}^2(\lambda)}, \quad (7)$$

where the instrumental width corresponds to the width of the Th-Ar lines.

These measurements can only be performed with best accuracy when the cometary oxygen lines are well separated from the telluric [OI] lines, i.e., when the geocentric velocities of the comet exceeds 15 km s⁻¹. Using the deblend function of the *splot* package in IRAF, we could measure the [OI] lines when the Doppler shift is as low as 7 km s⁻¹.

Comet	MJD	r (AU)	$\frac{I_{6300}}{I_{6364}}$	$\frac{I_{5577}}{I_{6300}+I_{6364}}$	FWHM _{intrinsic}		
					5577.339 Å	6300.304 Å	6363.776 Å
C/2002 V1 (NEAT)	2 647.037	1.22	3.10	0.06	2.08	1.57	1.40
C/2002 V1 (NEAT)	2 647.062	1.22	3.02	0.06	1.95	1.42	1.44
C/2002 V1 (NEAT)	2 649.031	1.18	3.05	0.07	2.23	1.45	1.42
C/2002 V1 (NEAT)	2 649.056	1.18	3.04	0.07	2.11	1.40	1.38
C/2002 V1 (NEAT)	2 719.985	1.01	3.05	0.10	2.76	1.54	1.49
C/2002 X5 (Kudo-Fujikawa)	2 705.017	1.06	2.97	0.10	2.64	1.46	1.50
C/2002 X5 (Kudo-Fujikawa)	2 705.039	1.07	2.98	0.10	2.61	1.54	1.60
C/2002 X5 (Kudo-Fujikawa)	2 705.060	1.07	3.01	0.10	2.64	1.50	1.54
C/2002 Y1 (Juels-Holvorcem)	2 788.395	1.14	2.93	0.09	2.88	1.52	1.47
C/2002 Y1 (Juels-Holvorcem)	2 788.416	1.14	3.01	0.09	2.75	1.54	1.49
C/2002 Y1 (Juels-Holvorcem)	2 789.394	1.16	2.98	0.11	3.09	1.59	1.57
C/2002 Y1 (Juels-Holvorcem)	2 789.415	1.16	3.01	0.10	3.03	1.61	1.59
C/2001 Q4 (NEAT)	2 883.293	3.73	2.95	0.33	2.51	2.39	2.39
C/2001 Q4 (NEAT)	2 883.349	3.73	3.22	0.33	2.31	2.63	2.69
C/2001 Q4 (NEAT)	2 889.236	3.67	3.17	-	-	2.49	2.52
C/2001 Q4 (NEAT)	2 889.320	3.66	3.51	0.30	2.55	2.75	2.36
C/2002 T7 (LINEAR)	3 131.421	0.68	3.04	0.14	3.12	1.82	1.80
C/2002 T7 (LINEAR)	3 151.976	0.94	3.51	0.11	2.84	1.70	1.71
C/2002 T7 (LINEAR)	3 152.036	0.94	3.39	0.09	2.81	1.66	1.72
C/2003 K4 (LINEAR)	3 131.342	2.61	3.08	0.10	2.51	1.81	1.66
C/2003 K4 (LINEAR)	3 132.343	2.59	3.13	0.08	2.76	2.12	1.94
C/2003 K4 (LINEAR)	3 329.344	1.20	3.20	0.07	2.38	1.52	1.52
9P/Tempel 1	3 553.955	1.51	3.06	0.05	2.91	1.61	1.43
9P/Tempel 1	3 554.954	1.51	3.00	0.04	2.14	1.59	1.48
9P/Tempel 1	3 555.955	1.51	3.00	-	-	1.56	1.46
9P/Tempel 1	3 557.007	1.51	3.05	0.05	2.03	1.55	1.44
9P/Tempel 1	3 557.955	1.51	3.23	0.03	1.75	1.54	1.47
9P/Tempel 1	3 558.952	1.51	3.23	0.04	1.79	1.58	1.48
9P/Tempel 1	3 559.954	1.51	3.21	0.05	2.57	1.84	1.60
9P/Tempel 1	3 560.952	1.51	3.17	0.06	2.77	1.72	1.52
9P/Tempel 1	3 561.953	1.51	3.18	0.04	1.92	1.63	1.48
9P/Tempel 1	3 562.956	1.51	3.25	0.03	1.67	1.61	1.48
73P-C/Schwassmann-Wachmann 3	3 882.367	0.95	3.24	0.11	2.12	1.31	1.30
73P-B/Schwassmann-Wachmann 3	3 898.369	0.94	3.03	0.11	2.46	1.54	1.48
8P/Tuttle	4 481.021	1.04	3.04	0.05	2.16	1.55	1.36
8P/Tuttle	4 493.018	1.03	3.03	0.04	2.21	1.55	1.41
8P/Tuttle	4 500.017	1.03	3.03	0.05	2.28	1.47	1.33
103P/Hartley 2	5 505.288	1.06	3.12	0.09	2.30	1.35	1.29
103P/Hartley 2	5 505.328	1.06	3.22	0.10	2.31	1.26	1.25
103P/Hartley 2	5 510.287	1.07	3.24	0.07	2.31	1.26	1.06
103P/Hartley 2	5 510.328	1.07	3.17	0.08	2.24	1.27	1.17
103P/Hartley 2	5 511.363	1.08	3.17	0.09	2.19	1.23	1.18
C/2009 P1 (Garradd)	5 692.383	3.25	2.92	0.21	2.28	1.67	1.87
C/2009 P1 (Garradd)	5 727.322	2.90	3.38	0.14	2.54	1.27	1.49
C/2009 P1 (Garradd)	5 767.278	2.52	3.12	0.10	2.19	1.30	1.31
C/2009 P1 (Garradd)	5 813.991	2.09	3.01	0.07	2.18	1.25	1.33
C/2009 P1 (Garradd)	5 814.974	2.08	3.07	0.07	2.16	1.33	1.33
C/2009 P1 (Garradd)	5 815.982	2.07	3.04	0.06	2.21	1.57	1.58

Table 4. Measured line ratios and velocity widths (km s⁻¹) for the three forbidden oxygen lines in the spectra of each comet. For the third spectrum of comets Q4 (NEAT) and Tempel 1, the green line couldn't be used because of a contamination by a cosmic ray.

5. Results

5.1. Intensity ratios

The two measured intensity ratios, I_{6300}/I_{6364} and $G/R = I_{5577}/(I_{6300} + I_{6364})$, are displayed for each spectrum in Fig. 5 and Fig. 6 respectively. When the collisional quenching is neglected, the intensity of a line is given by (Festou & Feldman 1981):

$$I = 10^{-6} \tau_p^{-1} \alpha \beta N \text{ photons cm}^{-2} \text{ s}^{-1} \quad (8)$$

where τ_p is the photo-dissociative lifetime of the parent, α is the yield of photo-dissociation, β corresponds to the branching ratio for the transition and N is the column density of the parent. Table 4 lists the results of the ratios for the 12 comets. The red doublet ratio is remarkably similar for all comets. The average value over the whole sample of spectra is 3.12 ± 0.02 . The error corresponds to the average sample standard deviation (σ/\sqrt{N}).

For a given comet, the dispersion of the ratio measurements from one spectrum to another is about 2 – 3%. This result is in very good agreement with the theoretical values of the branching ratio given by quantum mechanics, 3.096 by Galavis et al. (1997) and 2.997 by Storey & Zeippen (2000). Since both red lines are transitions from the same level to the ground state, τ_p , α and N in Eq. (8) are equal and the intensity ratio I_{6300}/I_{6364} is indeed equivalent to the branching ratio $\beta_{6300}/\beta_{6364}$. The ratio is also in agreement with the value of 3.09 ± 0.12 obtained by Cochran (2008) from a sample of 8 comets.

The G/R ratio has an average value of 0.11 ± 0.07 for the complete sample (see Fig. 6). The error corresponds to the sample standard deviation (σ) and will be given for the other average measurements. The dispersion of the ratio measurements for all spectra of a given comet is about 10 – 15%. This result is in agreement with the value of 0.09 ± 0.01 found by Cochran

(2008). This leads to the conclusion that H_2O is the main parent molecule producing oxygen atoms according to Bhardwaj & Raghuram (2012) values (Table 1).

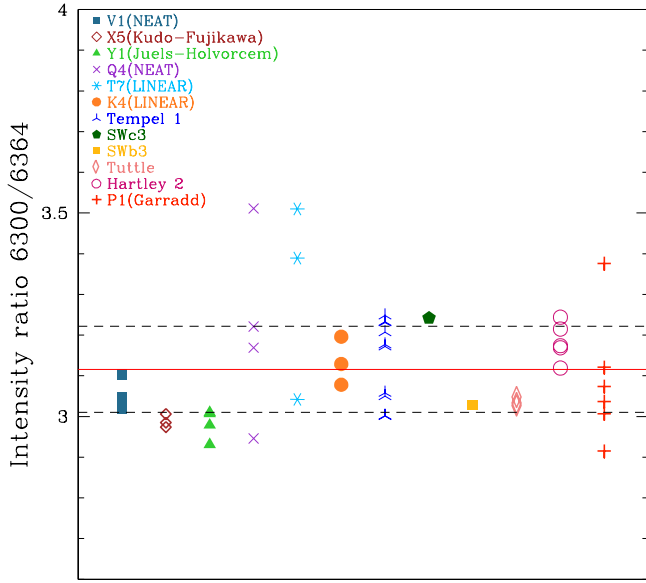


Fig. 5. The red doublet ratio for each comet. The spectra of a given comet have the same symbols. The average value of the sample (3.12 ± 0.11) is shown by the solid line. The dashed lines show the standard deviation (σ).

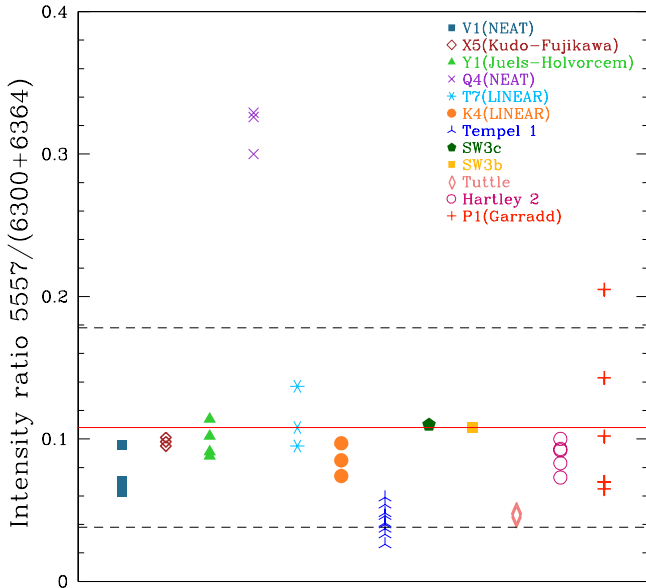


Fig. 6. Same figure as Fig. 5 for the G/R ratio. The mean value is 0.11 ± 0.07 . Note the data points for comet Q4 (NEAT) at 3.7 AU.

5.2. Line widths

Table 4 lists the intrinsic line velocity widths (FWHM (v)). The FWHM (v) is obtained from the $\text{FWHM}_{\text{intrinsic}}(\lambda)$ given in the Eq. 7 thanks to the relation :

$$\text{FWHM}(v) = \frac{\text{FWHM}_{\text{intrinsic}}(\lambda)}{\lambda_{[\text{OI}]} 2 \sqrt{\ln 2}}, \quad (9)$$

where $\lambda_{[\text{OI}]}$ corresponds to the wavelength of the considered oxygen line. The dispersion of the FWHM (v) for a given comet is about 5% for the red lines and 10% for the green line which is fainter. The two red lines widths are equal within the errors ($1.61 \pm 0.34 \text{ km s}^{-1}$ for the 6300 Å and $1.56 \pm 0.54 \text{ km s}^{-1}$ for the 6364 Å line) which is not a surprise since both lines are transitions from the O^1D state to the ground state (Fig. 7). This result is also consistent with the values of Cochran (2008) ($1.22 \pm 0.36 \text{ km s}^{-1}$). Figs. 8, 9 and 10 present the width of the three [OI] cometary lines, the three [OI] telluric lines and the width of some representative cometary lines in the vicinity. Those lines correspond to NH_2 lines in the red region and to C_2 lines in the green region. The widths of the red telluric lines are slightly smaller than the [OI] cometary lines ($1.37 \pm 0.35 \text{ km s}^{-1}$ for the 6300.304 Å line, $1.36 \pm 0.39 \text{ km s}^{-1}$ for the 6363.776 Å line) but their values are in quite good agreement with the cometary lines. Fig. 11 shows clearly that the [OI] cometary green lines are wider than the two red lines. Our mean value for the [OI] cometary green line is $2.44 \pm 0.28 \text{ km s}^{-1}$ (to be compared to $0.94 \pm 0.16 \text{ km s}^{-1}$ for C_2 lines and $0.90 \pm 0.37 \text{ km s}^{-1}$ for the green telluric line). This peculiarity was already noticed by Cochran (2008) who found a mean velocity of $2.49 \pm 0.36 \text{ km s}^{-1}$ in good agreement with our value. This width could be explained if the excess energy for the formation of the O^1S state is larger than for the O^1D state. Contrary to what is observed, theoretical models using Ly- α photons as excitation source give an excess velocity of 1.6 km s^{-1} for the O^1S state and a large value of 1.8 km s^{-1} for O^1D in the case of water photo-dissociation (Festou 1981).

6. Discussion

6.1. The G/R ratio at large heliocentric distance

In Fig. 6, we noticed that C/2001 Q4 (NEAT) has a G/R ratio of about 0.3 clearly such higher than other comets with values around 0.1. Q4 (NEAT) was at 3.7 AU from the Sun and this peculiarity led us to look more carefully on comets observed at large heliocentric distances (Fig. 12) (Decock et al. 2011).

If we only consider the data taken at $r < 2 \text{ AU}$, the G/R ratio average value is equal to 0.09 ± 0.02 which is in good agreement with the ratio obtained by Bhardwaj & Raghuram (2012) and Festou & Feldman (1981) for H_2O as the parent molecule (see Table 1). The large values of G/R in Q4 (NEAT) at 3.7 AU could be explained by the increasing contribution, at large heliocentric distances, of other parent molecules producing oxygen atoms. It is well known that the sublimation of H_2O significantly decreases beyond 3 AU while the sublimation of other ices like CO and/or CO_2 dominates comet activity (i.e., Crovisier & Encrenaz 2000). In order to investigate this hypothesis, we observed comet C/2009 P1 (Garradd) at four different heliocentric distances from 3.25 AU to 2.07 AU. Fig. 13 presents the G/R intensity ratios as a function of r for all spectra. A relation between the heliocentric distance and the G/R intensity ratio can be seen : the latter is getting rapidly larger when the comet is getting farther from the Sun. We added in this plot the Cochran & Cochran (2001) and

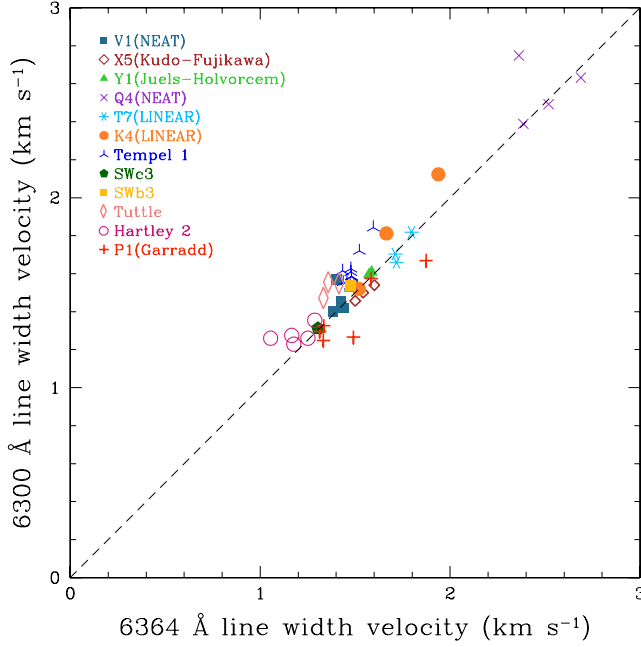


Fig. 7. The 6300.304 Å line width against the 6363.776 Å one. The different spectra for a given comet are denoted with the same symbol. Note the larger width for Q4 (NEAT).

Cochran (2008) average values coming from their sample of 8 comets. All these values are clumped around 1 AU with a ratio of ~ 0.1 . Q4 (NEAT) is one of their 8 comets and its G/R ratio is 0.09 ± 0.02 at $r = 0.98$ AU. A few other measurements found in the literature for comets observed at heliocentric distances beyond 2 AU were also added to the graph. Furusho et al. (2006) used the Subaru telescope to analyse the forbidden oxygen lines in comet 116P/Wild 4 observed at $r = 2.4$ AU. Capria et al. (2010) measured the intensity of these lines during and after the outburst of comet 17P/Holmes which occurred on October 24, 2007 when the comet was located at about $r = 2.5$ AU. McKay et al. (2012b) studied the [OI] lines of the two comets C/2006 W3 Christensen and C/2007 Q3 Siding Spring, respectively at 3.13 and 2.96 AU, with the ARCES echelle spectrometer of 3.5-m telescope at Apache Point Observatory. While the quality of the data are not as good because the lines are faint and sometimes heavily blended with the telluric line, all these measurements show a relatively high value of the G/R ratio when $r > 3$ AU. This confirms the hypothesis that oxygen is also coming from other molecules. CO and/or CO₂ are obvious candidates as they produce large values of the G/R ratio (see Table 1).

Using HST/STIS⁶ observations, Feldman et al. (2004) estimated at 4% the CO abundance relative to water in comet Q4 (NEAT) located at 1 AU from the Sun. The study made by Biver et al. (2012) on comet P1 (Garradd) provided an average value of 5% for the CO abundance when the comet was at 1.9 AU at pre-perihelion phase (October 2011). At large heliocentric distances, CO/H₂O had to be even higher. So the CO molecule could be a candidate to explain such a large G/R ratio. However, Bhardwaj & Raghuram (2012) showed that after the photo-dissociation of H₂O, the next main source for the green line emission is CO₂ with 10-40% abundance relative to water. They compared their model with the observational values obtained for C/1996 B2

⁶ HST/STIS is the acronym for Hubble Space Telescope / Space Telescope Imaging Spectrograph (<http://www.stsci.edu/hst/stis>).

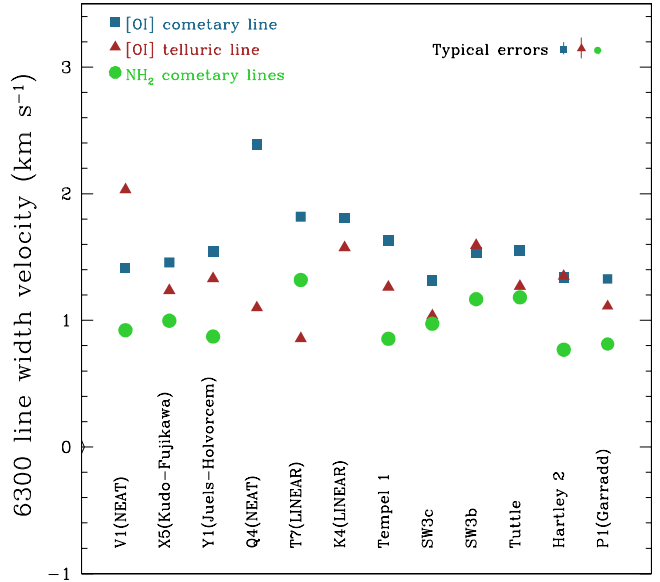


Fig. 8. The width velocity of the 6300.304 Å [OI] cometary line (■), the [OI] telluric line (▲) and nearby NH₂ cometary lines (●) (km s⁻¹) for one spectrum per comet. The typical errors correspond to the standard deviation (σ) obtained considering all the spectra of comet 8P/Tuttle. We have also checked this error by measuring randomly σ for a few spectra of other comets. For Q4 (NEAT) and K4 (LINEAR), the NH₂ cometary lines are missing because no lines were detected in this range.

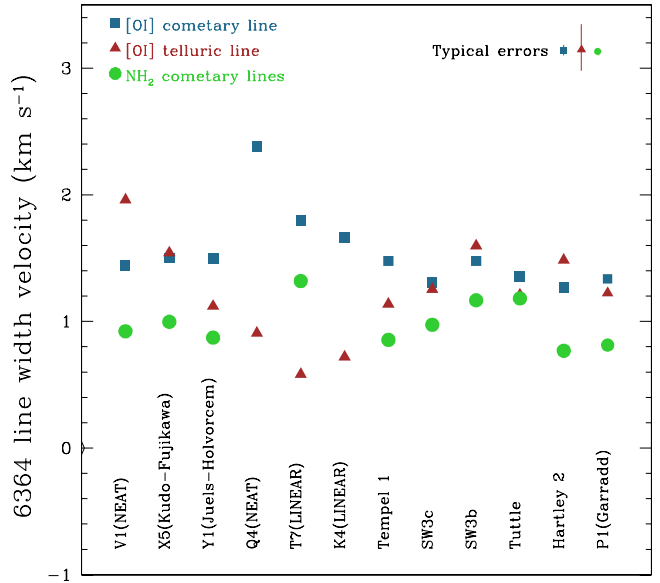


Fig. 9. Same figure as Fig. 8 for the 6363.776 Å line.

(Hyakutake) by Morrison et al. (1997) and Cochran (2008) when the comet was around 1 AU. Hyakutake is also rich in CO and its abundance was evaluated at 22% at 1 AU (Biver et al. 1999). Assuming a CO₂ abundance of 1% and a O(¹S) yield of 0.2%, Bhardwaj & Raghuram (2012) concluded that the production rates of the O(¹S) are similar for CO and CO₂ ($\sim 10 - 25\%$) with

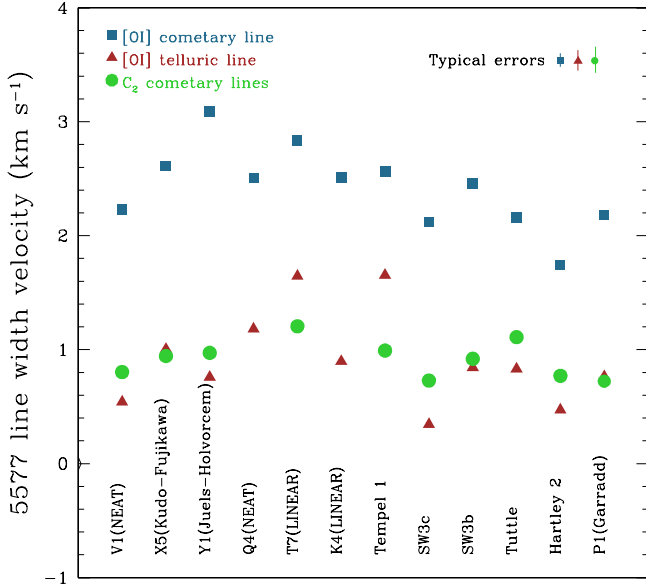


Fig. 10. Same figure as Fig. 8 for the 5577.339 Å line and with C₂ cometary lines. The larger width, by about 1 km s⁻¹, of the [OI] cometary green line is obvious.

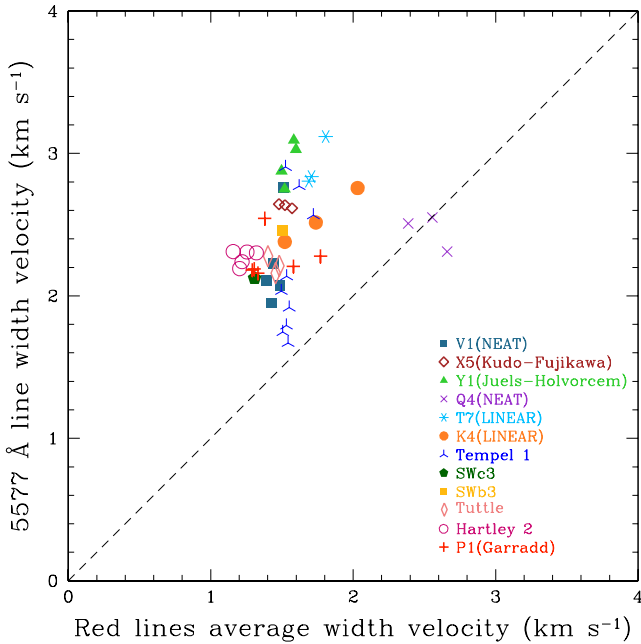


Fig. 11. The 5577.339 Å line width against the average width of the red lines. The different spectra of a given comet are denoted with the same symbol. Note that the green line is always larger than the red lines except for Q4 (NEAT).

such abundances. Therefore, since Q4 (NEAT) and P1 (Garradd) have less CO than Hyakutake, CO₂ molecules could rather be the main contributor to the formation of the green line emission for these two comets observed at large heliocentric distance. CO₂ measurements are unfortunately very rare because they are difficult to obtain to confirm this hypothesis. But if this is the case, G/R ratios estimated might be used as a proxy for the CO₂ rela-

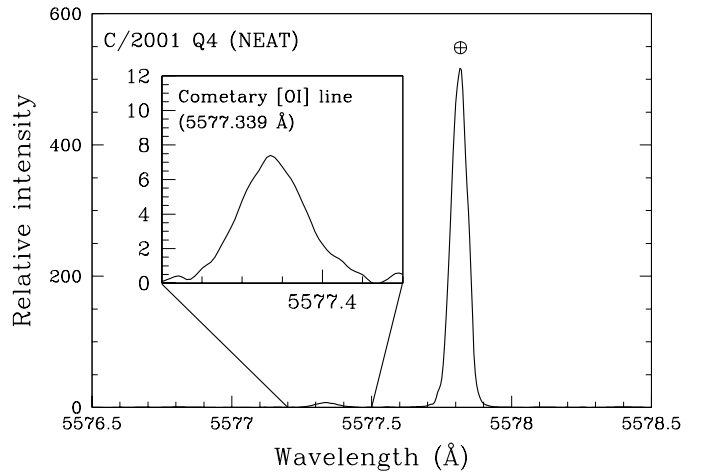
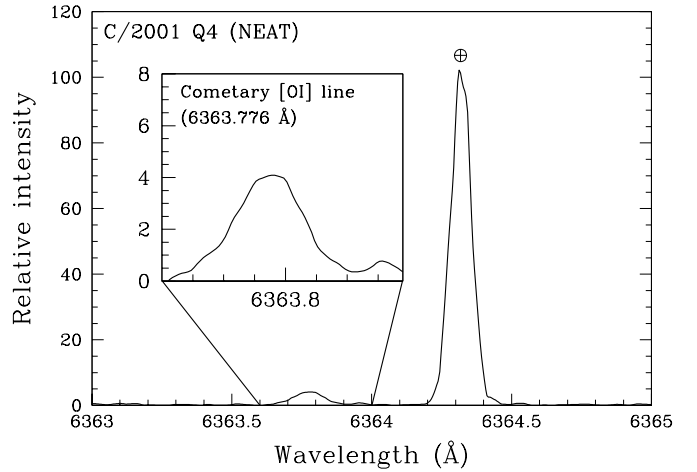
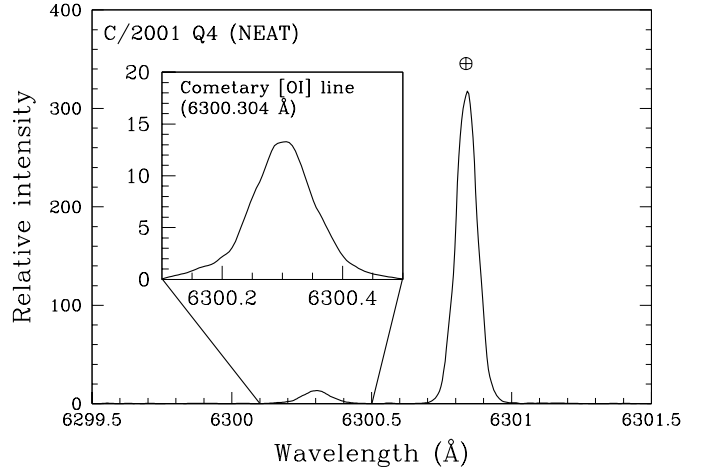


Fig. 12. These two hours spectra of comet Q4 (NEAT) obtained with the ESO VLT are the most distant detection of [OI] lines in a comet (at 3.7 AU). The lines are well detected and well separated from the telluric line. The width of the green and the red lines are the same.

tive abundance but such a relation should be carefully calibrated on a sample of comets with known CO₂, as also suggested by McKay et al. (2012a).

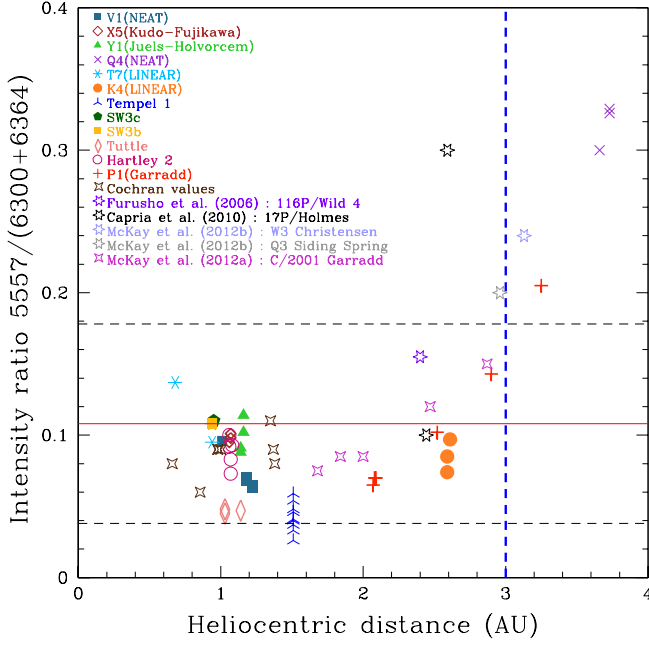


Fig. 13. The G/R intensity ratio as a function of the heliocentric distance (AU). The same symbol is used for the different spectra of each comet. The most distant comets have a higher ratio. Other values from the literature are also plotted. The solid line represents the average value only for our sample of spectra and the standard deviation (σ) range is denoted with horizontal dashed lines. If we only consider the data at $r < 2$ AU, the average value of G/R ratio is 0.09 ± 0.02 . The vertical dashed line at 3 AU represents the distance out to which the sublimation of water is strongly decreasing (Crovisier & Encrenaz 2000).

Using Eq. 8 and only considering the main parent species of oxygen atoms (i.e H_2O , CO_2 and CO), we can write the G/R ratio as :

$$G/R = \frac{I_{\text{green}}}{I_{\text{red}}} = \frac{W_{\text{H}_2\text{O}}^{\text{green}} \beta^{\text{green}} N_{\text{H}_2\text{O}} + W_{\text{CO}_2}^{\text{green}} \beta^{\text{green}} N_{\text{CO}_2} + W_{\text{CO}}^{\text{green}} \beta^{\text{green}} N_{\text{CO}}}{W_{\text{H}_2\text{O}}^{\text{red}} \beta^{\text{red}} N_{\text{H}_2\text{O}} + W_{\text{CO}_2}^{\text{red}} \beta^{\text{red}} N_{\text{CO}_2} + W_{\text{CO}}^{\text{red}} \beta^{\text{red}} N_{\text{CO}}}. \quad (10)$$

where $W_b^a = \alpha_b^a \tau_b^{-1}$ corresponds to the effective production rates of $\text{O}(^1\text{S})$ and $\text{O}(^1\text{D})$ states⁷. However, if we consider that oxygen atoms only come from H_2O and CO molecules, we found that G/R ratio does not change strongly : it varies from 0.08 to 0.1 for a CO abundance between 10% and 80%. Therefore, we assume that the [OI] atoms are only produced by the H_2O and CO_2 photo-dissociations. Hence, Eq. 10 can be simplified as :

$$G/R = \frac{I_{\text{green}}}{I_{\text{red}}} = \frac{W_{\text{H}_2\text{O}}^{\text{green}} \beta^{\text{green}} N_{\text{H}_2\text{O}} + W_{\text{CO}_2}^{\text{green}} \beta^{\text{green}} N_{\text{CO}_2}}{W_{\text{H}_2\text{O}}^{\text{red}} \beta^{\text{red}} N_{\text{H}_2\text{O}} + W_{\text{CO}_2}^{\text{red}} \beta^{\text{red}} N_{\text{CO}_2}} \quad (11)$$

Therefore, the $\text{CO}_2/\text{H}_2\text{O}$ abundance can be computed by :

$$\frac{N_{\text{CO}_2}}{N_{\text{H}_2\text{O}}} = \frac{(G/R) W_{\text{H}_2\text{O}}^{\text{red}} - \beta^{\text{green}} W_{\text{H}_2\text{O}}^{\text{green}}}{\beta^{\text{green}} W_{\text{CO}_2}^{\text{green}} - (G/R) W_{\text{CO}_2}^{\text{red}}}. \quad (12)$$

⁷ The production rates W_b^a are given in Tables 1 and 2 of Bhardwaj & Raghuram (2012) (i.e $W_{\text{H}_2\text{O}}^{\text{red}} = 8 \cdot 10^{-7} \text{ s}^{-1}$, $W_{\text{H}_2\text{O}}^{\text{green}} = 6.4 \cdot 10^{-8} \text{ s}^{-1}$, $W_{\text{CO}_2}^{\text{green}} = 7.2 \cdot 10^{-7} \text{ s}^{-1}$, $W_{\text{CO}_2}^{\text{red}} = 1.2 \cdot 10^{-6} \text{ s}^{-1}$, $W_{\text{CO}}^{\text{green}} = 4 \cdot 10^{-8} \text{ s}^{-1}$ and $W_{\text{CO}}^{\text{red}} = 5.1 \cdot 10^{-8} \text{ s}^{-1}$) and $\beta^{\text{green}} = 0.91$ (Slanger et al. 2006).

The W_b^a are independent of the heliocentric distance because all of them depend on the same heliocentric distance. This is also the case for the values given in Table 1. Considering the same values for W_b^a and β^{green} , we also computed the $\text{CO}_2/\text{H}_2\text{O}$ abundance from the G/R ratios of comets Q4 (NEAT) and P1 (Garradd) measured by Cochran (2008) and McKay et al. (2012a), respectively. From our data, we find an exponential relation between the $\text{CO}_2/\text{H}_2\text{O}$ abundance and the heliocentric distance of the type $\text{CO}_2/\text{H}_2\text{O} = A e^{br}$ with $A = 1 \cdot 10^{-4}$ and $b = 2.41$. These results are shown in Fig. 14. We noticed that $\text{CO}_2/\text{H}_2\text{O}$ is as high as 75% in Q4 (NEAT) and that CO_2 starts to contribute to the G/R ratio at 2.5 AU in the comets.

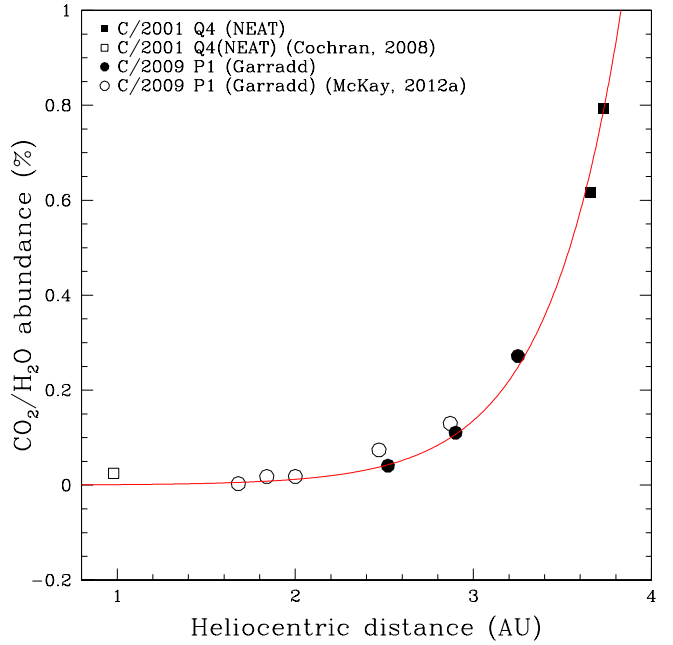


Fig. 14. Evolution of the $\text{CO}_2/\text{H}_2\text{O}$ abundance as a function of the heliocentric distance (AU). Assuming that a bigger G/R ratio comes from a more important contribution of CO_2 for large heliocentric distance comets, measuring this ratio can give us the CO_2 abundance from ground observations. The curve corresponds to an exponential fit of our data (■ and ●).

Therefore, the forbidden oxygen lines measurement could become a new way to determine the CO_2 abundance in comets at different heliocentric distances from ground observations while the direct measurement of CO_2 molecules is only possible from space.

6.2. The [OI] lines widths

One explanation for the large width of the [OI] green line could be that exciting photons producing oxygen atoms in the ^1S state have more energy than the Lyman α photons and/or come from an other parent molecule. Indeed, Fig. 7 of Bhardwaj & Raghuram (2012) shows that the wavelength region for the major production of $\text{O}(^1\text{S})$ coming from CO_2 seems to be the 955-1165 Å band. New theoretical studies could be necessary to evaluate the excess velocity for the $\text{O}(^1\text{S})$ state coming from the photo-dissociations of both H_2O and CO_2 .

In Fig. 11, we also notice that the [OI] red lines of the comet Q4 (NEAT) are wider than in other comets while the width

MJD	r(AU)	G/R	N_{CO_2}/N_{H_2O}
5 505.288	1.06	0.09	0.028
5 505.328	1.06	0.10	0.040
5 510.287	1.07	0.07	0.001
5 510.328	1.07	0.08	0.015
5 511.363	1.08	0.09	0.030

Table 5. The CO_2/H_2O abundances estimated from Eq. 12 for the comet 103P/Hartley 2.

of the green line is normal with respect to other comets. This peculiarity seems real as both red lines show the same width and they are $2\text{-}\sigma$ away from the average value of the sample ($1.58 \pm 0.30 \text{ km s}^{-1}$). Moreover, the telluric lines in Q4 (NEAT) have the usual width ($0.99 \pm 0.10 \text{ km s}^{-1}$ for the 6300 \AA line, $0.87 \pm 0.04 \text{ km s}^{-1}$ for the 6364 \AA line and $0.80 \pm 0.26 \text{ km s}^{-1}$ for the green line) which discards a problem with the spectra or the analysis. The width of the red lines and the green line is similar in this unique case ($2.57 \pm 0.16 \text{ km s}^{-1}$ for the 6300 \AA line, $2.49 \pm 0.15 \text{ km s}^{-1}$ for the 6364 \AA and $2.46 \pm 0.13 \text{ km s}^{-1}$ for the 5577 \AA line) and could give us clues about the process at play. As previously discussed, at large heliocentric distances, the [OI] lines could mainly come from the CO_2 molecules which preferentially photo-dissociate in the 1S state while at low heliocentric distances, they essentially come from H_2O which preferentially dissociates in the 1D state (Table 1). This means that at large distances, the red lines are mainly produced through the $^1S\text{-}^1D$ channel which also produces the green line, while at low distances as H_2O dominates they are mostly produced directly from the 1D state. We thus expect the widths of the red and green lines to be similar at high distances because the $O(^1S)$ and $O(^1D)$ atoms are mostly produced from a same molecule, while they can differ at low distances, as observed. CO_2 is the best candidate and the larger width could be explained by the main excitation source of CO_2 , the $955\text{-}1165 \text{ \AA}$ band, which is more energetic than $Ly\text{-}\alpha$ photons, as shown in Fig. 11 of Bhardwaj & Raghuram (2012). This peculiarity is not seen for comet P1 (Garradd) maybe because the spectrum is not taken at sufficiently large heliocentric distance and CO_2 abundance was lower than in Q4 (NEAT). Anyway, this hypothesis needs to be confirmed by observing other comets at large heliocentric distances ($> 3.5 \text{ AU}$).

6.3. 103P/Hartley 2

The Jupiter Family comet 103P/Hartley 2 has been found rich in CO_2 ($\sim 20\%$) from EPOXI measurements (A'Hearn et al. 2011) and poor in CO (Weaver et al. 2011). Thanks to the Eq. 12, we could evaluate the CO_2 abundances from our G/R ratios measured at $\sim 1 \text{ AU}$ and compare them with the values obtained by EPOXI. The results are given in Table 5. The mean G/R ratio of 0.09 ± 0.01 is similar to those of other comets observed below 2.5 AU and give a relative abundance of CO_2 of only $\sim 3\%$ while a G/R ratio of ~ 0.2 would be needed to reach a CO_2 abundance as high as $\sim 20\%$.

We do not confirm a high value for 103P/Hartley 2 as claimed by (McKay et al. 2012) or a large dispersion in the abundances. Their values might be higher because they used a $W_{H_2O}^{green}$ of Bhardwaj & Raghuram (2012) equal to $2.6 \cdot 10^{-8} \text{ s}^{-1}$ while the value provided in Table 1 of this paper is $6.4 \cdot 10^{-8} \text{ s}^{-1}$.

The discrepancy with the EPOXI CO_2 abundance is interesting. Below 2.5 AU , G/R values are distributed from 0.05 for comets like 9P/Tempel 1 and 8P/Tuttle and can go up to 0.12 for

T7 (LINEAR). The spread from comet to comet is higher than the errors estimated from the dispersion from the spectra of a same comet which could be explained by an intrinsic variation of G/R from comet to comet due to the content of CO_2 . The G/R range, of the order of 0.1 (implying a CO_2 variation of $\sim 20\%$) is of the same order as the range of CO_2 abundance in comets of various origins measured below 2.5 AU (A'Hearn 2012).

The fact that some comets, like 9P/Tempel 1 and 8P/Tuttle, have values lower than the pure water case (giving a $G/R_{min} = 0.08$ from Bhardwaj & Raghuram (2012)) and that the 103P/Hartley 2 G/R ratio is too low compared to EPOXI CO_2 abundances, could indicate a problem with the models. The pure water ratio should be 0.05 or lower based on the comets with the smallest values (9P/Tempel 1 has a CO_2 abundance of $\sim 7\%$ (Feaga et al. (2007a), Feaga et al. (2007b))). Bhardwaj & Raghuram (2012) tried $\alpha_{H_2O}^{green}$ values from 0% to 1% and finally chose 1%, but this value is uncertain. Without CO_2 , $G/R_{min} = \beta_{H_2O}^{green} W_{H_2O}^{green} / W_{H_2O}^{red}$. If we use 0.5% for $\alpha_{H_2O}^{green}$, G/R_{min} is equal to 0.04 instead of 0.08 which would be in better agreement with our smallest values.

6.4. Deep Impact

The spectra of comet 9P/Tempel 1 were analysed before and after the July 4 collision with the Deep Impact spacecraft. No difference was observed in the intensity ratios and the lines widths before and after the impact (Fig. 15). We have no spectrum during the impact. The first spectrum after the impact was taken at 53559.954 UT (i.e. ~ 6 hours after the impact). Cochran (2008) did not notice any change during the impact either.

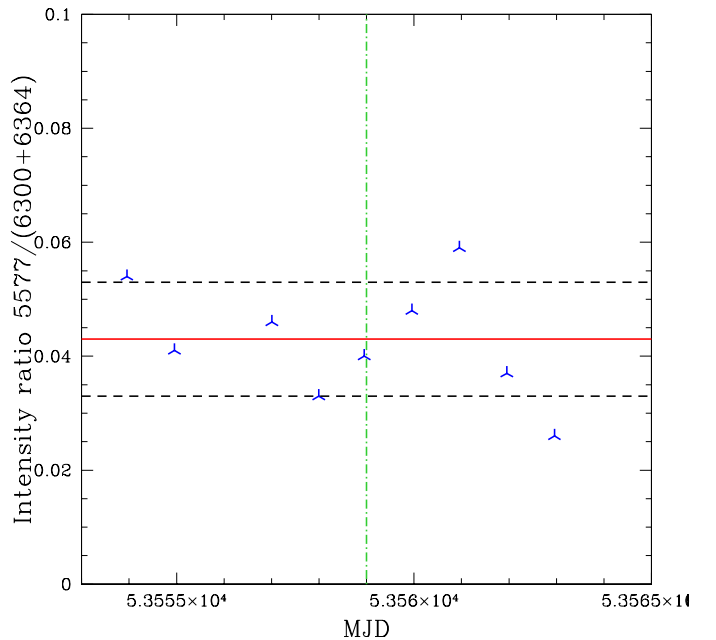


Fig. 15. The G/R intensity ratio of comet 9P/Tempel 1 from MJD 53553.955 to 53562.956 UT. The Deep Impact event corresponds to the vertical line (53559 UT). The average value is shown by the solid red line and the dashed lines correspond to the standard deviation (σ). The mean value around the impact (from 53553.955 UT to 53562.956 UT) is 0.04 ± 0.01 . No variation of the ratio was noticed after the impact.

6.5. Solar activity

Our data were obtained over the 23th solar cycle characterized by its maximum of activity in 2001 and its minimum activity in 2008. Despite the decrease of the solar activity during the observations of C/2001 V1 (NEAT) and 8P/Tuttle, no change in the intensities and widths of lines were noticed. Solar activity does not appear to have any influence on the results of our work.

7. Conclusion

From January 2003 to September 2011, 12 comets of various origins were observed at different heliocentric distances and 48 high resolution spectra were obtained with the UVES spectrograph at VLT (ESO). Within this whole sample, we observed the three [OI] forbidden oxygen lines with high resolution and signal to noise and we measured the intensity ratios (I_{6300}/I_{6364} and $G/R = I_{5577}/(I_{6300} + I_{6364})$) as well as the FWHM (v) of the lines. The results can be summarized as follows :

1. The I_{6300}/I_{6364} ratio (3.12 ± 0.02) is in very good agreement with the branching ratio obtained by quantum mechanics, especially the work done by Galavis et al. (1997). This result shows the high quality of our measurements.
2. From theoretical values given in Table 1, the G/R ratio for comets observed below 2 AU (0.09 ± 0.02) confirms H₂O as the main parent molecule photo-dissociating to produce oxygen atoms. However, when the comet is located at larger heliocentric distances ($r \geq 2.5$ AU), the ratio increases rapidly showing that an other parent molecule is contributing. We have shown that CO₂ is the best candidate. Measuring the G/R ratios could then be a new way to estimate the abundances of CO₂, a very difficult task from the ground. Assuming that only the photo-dissociation of H₂O and CO₂ produce [OI], we found a relation between CO₂ abundance and the heliocentric distance of the comet. The Q4 (NEAT) abundance of CO₂ at 3.7 AU is found to be ~75%.
3. The intrinsic green line width is wider than the red ones by about 1 km s^{-1} . Theoretical estimations considering Ly- α as the only excitation source for the two states lead to the conclusion that the excess energy for O(¹D) is larger than for O(¹S) which is in contradiction with our observations. This discrepancy might be explained by a different nature of the excitation source and/or a contribution of CO₂ as parent molecule to the O(¹S) state. Indeed, Bhardwaj & Raghuram (2012) have shown that for the photo-dissociation of CO₂, the main excitation source might rather be the 995-1165 Å band. To check this hypothesis quantitatively, it would be necessary to estimate theoretically the excess energy for the oxygen atoms when the wavelength band is 995-1165 Å, accounting for the photo-dissociation of both H₂O and CO₂. The widths of the three [OI] lines are similar in Q4 (NEAT) at ~ 3.7 AU. This could be in agreement with CO₂ being the main contributor for the three [OI] lines at large heliocentric distance. Other comets at large r have to be observed to test this hypothesis.
4. More CO₂ (and CO) abundance determinations, together with G/R oxygen ratios and line widths at different heliocentric distances, are clearly needed in order to give a general conclusion about the oxygen parent molecule.
5. The CO₂ rich comet 103P/Hartley 2 (~ 20%) does not present a high G/R ratio normally expected from Eq. 12. We suggest a new value of 0.5% for $\alpha_{\text{H}_2\text{O}}^{\text{green}}$ that could also explain

the low values of G/R obtained for comets 9P/Tempel 1 and 8P/Tuttle.

Acknowledgements. A.D thanks the support of the Belgian National Science Foundation F.R.I.A., Fonds pour la formation à la Recherche dans l'Industrie et l'Agriculture. E.J. is Research Associate FNRS, J.M. is Research Director FNRS and D.H. is Senior Research Associate FNRS.

C. Arpigny is acknowledged for the helpful discussions and constructive comments.

References

- A'Hearn, M. F. 2012, in American Astronomical Society Meeting Abstracts, Vol. 220, American Astronomical Society Meeting Abstracts #220, 120.04
- A'Hearn, M. F., Belton, M. J. S., Delamere, W. A., et al. 2011, *Science*, 332, 1396
- Bhardwaj, A. & Raghuram, S. 2012, *ApJ*, 748, 13
- Biver, N., Bockelée-Morvan, D., Crovisier, J., et al. 1999, *AJ*, 118, 1850
- Biver, N., Bockelée-Morvan, D., Lis, D. C., et al. 2012, *LPI Contributions*, 1667, 6330
- Capria, M. T., Cremonese, G., & de Sanctis, M. C. 2010, *A&A*, 522, A82
- Cochran, A. L. 2008, *Icarus*, 198, 181
- Cochran, A. L. & Cochran, W. D. 2001, *Icarus*, 154, 381
- Crovisier, J. & Encrenaz, T., eds. 2000, *Comet science : the study of remnants from the birth of the solar system*
- Decock, A., Jehin, E., Manfroid, J., & Hutsemékers, D. 2011, in EPSC-DPS Joint Meeting 2011, 1126
- Dekker, H., D'Odorico, S., Kaufer, A., Delabre, B., & Kotzlowski, H. 2000, in Presented at the Society of Photo-Optical Instrumentation Engineers (SPIE) Conference, Vol. 4008, Society of Photo-Optical Instrumentation Engineers (SPIE) Conference Series, ed. M. Iye & A. F. Moorwood, 534–545
- Ehrenfreund, P. & Charnley, S. B. 2000, *ARA&A*, 38, 427
- Feaga, L. M., A'Hearn, M. F., Sunshine, J. M., Groussin, O., & Farnham, T. L. 2007a, *Icarus*, 190, 345
- Feaga, L. M., A'Hearn, M. F., Sunshine, J. M., Groussin, O., & Farnham, T. L. 2007b, *Icarus*, 191, 134
- Feldman, P. D., Weaver, H. A., Christian, D., et al. 2004, in Bulletin of the American Astronomical Society, Vol. 36, AAS/Division for Planetary Sciences Meeting Abstracts #36, 1121
- Festou, M. & Feldman, P. D. 1981, *A&A*, 103, 154
- Festou, M. C. 1981, *A&A*, 96, 52
- Furusho, R., Kawakita, H., Fuse, T., & Watanabe, J. 2006, *Advances in Space Research*, 38, 1983
- Galavis, M. E., Mendoza, C., & Zeppen, C. J. 1997, *A&AS*, 123, 159
- Huebner, W. F. & Carpenter, C. W. 1979, *NASA STI/Recon Technical Report N*, 80, 24243
- Jehin, E., Manfroid, J., Hutsemékers, D., Arpigny, C., & Zucconi, J.-M. 2009, *Earth Moon and Planets*, 105, 167
- Levison, H. F. 1996, in *Astronomical Society of the Pacific Conference Series*, Vol. 107, *Completing the Inventory of the Solar System*, ed. T. Rettig & J. M. Hahn, 173–191
- Manfroid, J., Jehin, E., Hutsemékers, D., et al. 2009, *A&A*, 503, 613
- McKay, A. J., Chanover, N. J., DiSanti, M. A., et al. 2012a, *LPI Contributions*, 1667, 6212
- McKay, A. J., Chanover, N. J., Morgenthaler, J. P., et al. 2012b, *Icarus*, 220, 277
- McKay, A. J., Chanover, N. J., Morgenthaler, J. P., et al. 2012, *Icarus*, <http://dx.doi.org/10.1016/j.icarus.2012.06.020>, in press
- Morrison, N. D., Knauth, D. C., Mulliss, C. L., & Lee, W. 1997, *PASP*, 109, 676
- Slinger, T. G., Cosby, P. C., Sharpee, B. D., Minschwaner, K. R., & Siskind, D. E. 2006, *Journal of Geophysical Research (Space Physics)*, 111, 12318
- Storey, P. J. & Zeppen, C. J. 2000, *MNRAS*, 312, 813
- Swings, P. 1962, *Annales d'Astrophysique*, 25, 165
- Weaver, H. A., Feldman, P. D., A'Hearn, M. F., Dello Russo, N., & Stern, S. A. 2011, *ApJ*, 734, L5